

Optical response of carbon nanotubes functionalized with (free-base, Zn) porphyrins, and phthalocyanines: A DFT study

J. D. Correa and W. Orellana

Departamento de Ciencias Físicas, Universidad Andres Bello, Av. República 220, 837-0134 Santiago, Chile

(Received 30 June 2012; published 10 September 2012)

We use density-functional theory calculations to study the stability, electronic, and optical properties of free-base and Zn porphyrins and phthalocyanines (H_2P , H_2Pc , ZnP , and $ZnPc$) noncovalently attached onto a semiconducting carbon nanotube (CNT). The macrocycle physisorption is described by van der Waals density functional while optical response is obtained through the imaginary part of the dielectric function. Our results show a rather strong macrocycle binding energy, ranging from 1.0 to 1.5 eV, whereas the CNT geometry and electronic properties are weakly affected by the adsorbates. The optical spectrum shows that CNT-porphyrins and CNT-phthalocyanines assemblies would absorb at different energies of the visible solar radiation spectrum, which would increase the conversion energy efficiency in a photovoltaic device including both macrocycles.

DOI: [10.1103/PhysRevB.86.125417](https://doi.org/10.1103/PhysRevB.86.125417)

PACS number(s): 78.67.Ch, 71.35.Cc, 78.40.Ri, 68.43.Bc

I. INTRODUCTION

The functionalization of single-walled carbon nanotubes (CNTs) with organic molecules is currently the subject of intense theoretical and experimental research exploring functional materials for light-harvesting applications^{1,2} and catalysis.³⁻⁵ Particularly, inorganic-organic hybrid compounds involving CNTs and planar electron-rich aromatic macrocycles like porphyrins and phthalocyanines, which are characterized by a strong absorption in the visible and ultraviolet spectra, have attracted great interest envisioning CNT-based photovoltaic devices.^{1,6,7} Indeed, recent experiments on CNTs functionalized noncovalently with free-base porphyrins and metalloporphyrins have shown large ultrafast nonlinear absorption,⁸ as well as highly efficient excitation energy transfer.⁹ These reports suggest that molecular assemblies may be used as controllable electron donor-acceptor nano hybrids while preserving the nanotube intrinsic properties.¹⁰ Although the above mentioned experiments indicate that π - π stacking or van der Waals interaction are responsible for the macrocycles attachment onto the CNT, little is known about the theoretical characterization of the electronic and optical properties observed on these complexes and the role played by the dispersive forces.

Recently, accurate optical response calculations based on many-body perturbation theory, namely GW approximation and the Bethe-Salpeter equation (BSE), have been performed for porphyrins and phthalocyanines in the gas phase.¹¹⁻¹⁴ Although they give excellent results for the evaluation of frontier orbitals and optical absorption spectra of such molecules, at this moment these techniques are prohibitive for extended systems like molecules adsorbed on CNTs due to the computational costs. Alternatively, most calculations in extended systems involving CNTs report linear optical response neglecting many-body effects.¹⁵⁻¹⁷ However, theoretical and experimental results have established that many-body interactions shift the CNT bandgap to higher energies and create excitons with large binding energies, which vary inversely with the CNT diameters.^{18,19} In addition, recent scanning tunneling spectroscopy measurements have proposed that exciton binding energies can be deduced by the difference between the intrinsic CNT bandgap and the optical transition, taking values as high as 0.4 eV.²⁰

Optical experiments have also shown that the interaction of CNT with physisorbed molecules and other CNTs leads to redshifts in the optical transition of about 10 meV.^{21,22} A recent microscopic model predicts the same redshift in both excitonic and free-particle absorption spectra, which is attributed to an efficient coupling between charge carrier and the molecular dipole field.² In addition, many-body calculations have suggested that this redshift results from the local polarizability induced by the adsorbates,²³ in close agreement with experiments.²⁰ In this work we address the same problem but considering (free-base and Zn) porphyrins and phthalocyanines macrocycles as adsorbates, using van der Waals density functional to model dispersive interactions. The response of the functionalized CNT to light polarized both parallel and perpendicular with respect to the CNT axis is investigated through the imaginary part of the dielectric function, revealing redshifts in the optical absorption, in close agreement with the above results. Although our approach does not consider many-body interactions due to the system size, it gives qualitatively good results that allows us to extract relevant information about the optical absorption of CNT-macrocycle complexes for photovoltaic applications.

II. THEORETICAL APPROACH

Our DFT calculations were carried out by using the SIESTA *ab initio* package,²⁴ which employ norm-conserving pseudopotentials and localized atomic orbitals as basis set (double- ζ , singly polarized in the present work). The macrocycles physisorption on the CNT sidewall is assessed by van der Waals density functional as proposed by Dion *et al.*²⁵ This approach has been successfully applied to describe the dispersive interaction of aromatic molecules on graphite and CNTs.^{26,27} In the present work we consider a semiconducting (14,0) CNT with a diameter of 1.1 nm, and four macrocycles: Zn-porphyrin (ZnP), Zn-phthalocyanine (ZnPc), free-base porphyrin (H_2P), and free-base phthalocyanine (H_2Pc).

The macrocycle adsorption on the CNT surface is studied within the supercell approach with periodic boundary conditions along the nanotube axis (y direction) with unit-cell lengths of $4a_0$ and $6a_0$ for the CNT-porphyrin and

CNT-phthalocyanine complexes, respectively, where $a_0 = 2.49 \text{ \AA}$. In order to avoid interaction between CNT images, the lateral separation between them is fixed to be of 10 \AA . For the Brillouin zone sampling we used a $1 \times 3 \times 1$ Monkhorst-Pack mesh. Tests of convergence were performed considering a larger mesh ($1 \times 5 \times 1$), our results show differences in the total energy less than 0.01 eV . In addition, band structure calculations obtained with both meshes show negligible differences. For the optical calculations, we used $1 \times 31 \times 1$ and $1 \times 51 \times 1$ k -points meshes for the CNT-porphyrins and CNT-phthalocyanines, respectively. The macrocycle binding energies were calculated by the energy difference between adsorbed and separated constituents, considering corrections due to the basis set superposition error. The complexes were fully relaxed by conjugate gradient minimization until the forces on the atoms were less than 0.05 eV/\AA . Three positions for the H_2P and H_2Pc adsorption on the CNT surface were considered: In position I the N-H bonds are perpendicular to the CNT axis, in position II the N-H bonds are parallel to the CNT axis, and in position III the N-H bonds form an angle of 45° with respect to the CNT axis. For ZnP and ZnPc, positions I and II are equivalent by symmetry.

The optical spectrum is obtained through the imaginary part of the dielectric function in the linear-optical-response approximation, according to the equation:

$$\varepsilon_2(\omega) = A \int d\mathbf{k} \sum_{c,v} |\hat{\mathbf{e}} \cdot \langle \Psi_c(\mathbf{k}) | \mathbf{r} | \Psi_v(\mathbf{k}) \rangle|^2 \delta(E_c - E_v - \hbar\omega). \quad (1)$$

Here, A is a constant that depends on the cell sizes; Ψ_c and Ψ_v are the occupied and empty Kohn-Sham orbitals. The delta function represents the conservation of energy, which are described by Gaussian function with a smearing of 0.06 eV .

Optical properties of CNTs are dominated by transitions between corresponding van Hove peaks on opposite sides of the Fermi energy (E_{ii}). Weisman and Bachilo plotting spectrofluorimetric data against the nanotube diameters predict first (E_{11}) and second (E_{22}) van Hove optical transitions for a wide range of semiconducting CNTs.²⁸ For the (14,0) CNT they obtained a first optical transition of $E_{11} = 0.96 \text{ eV}$, whereas our calculations give a value of 0.71 eV . The difference (0.25 eV) is attributed to the many-body effects, which are neglected in our calculation, as discussed above. To verify this we use the empirical relation derived by Dukovic *et al.* that estimates the band gap redshift associated to many-body effects, given by $\Delta E_{11} = 0.34 \text{ eV}/d$, where d is the CNT diameter.¹⁹ For our semiconducting (14,0) CNT ($d = 1.1 \text{ nm}$), we find $\Delta E_{11} = 0.31 \text{ eV}$. According to recent experiments, this energy can be associated to the exciton binding energy in the (14,0) CNT.²⁰

III. RESULTS AND DISCUSSION

A. Structural and electronic properties

Figure 1 shows the equilibrium geometries of the free-base porphyrin and phthalocyanine adsorbed on the CNT sidewall at position III. We observe a strong deformation for the phthalocyanine, which tends to adopt the CNT curvature,

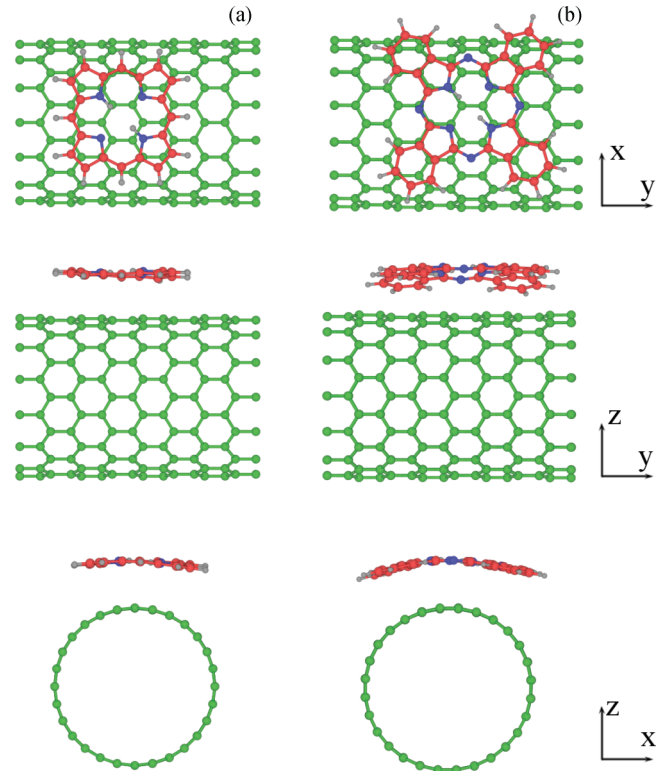


FIG. 1. (Color online) Equilibrium geometries of the free-base porphyrin (a) and the free-base phthalocyanine (b) in the adsorption position II. Green and red balls represent C atoms of the CNT and the macrocycles, respectively. Blue and gray balls represent N and H atoms.

while for porphyrin only a small twist is found. The respective binding energy of these macrocycles are found to be around 1.5 and 1.0 eV , suggesting that the strength of the CNT-macrocycle interaction is quite strong with a clear dependence on the contact area of the complex. In fact, if we consider the macrocycle physisorption energy per unit length of contact, this has the same order of the CNT chemisorption energy on a silicon surface.²⁹ Similar results for the strong molecular physisorption have been found in previous calculations of benzene and naphthalene on graphite using the same theoretical approach of the present work, which also agree well with the available experimental data.²⁶ Table I lists macrocycle binding energies and adsorption distances from the CNT surfaces. The Zn macrocycles show binding energies slightly higher than their free-base counterpart (less than 0.06 eV), suggesting that the macrocycle size (instead of metal center) is the relevant

TABLE I. Binding energy (E_b) and adsorption distance (d) for the macrocycles adsorbed on the CNT at positions I, II, and III.

Complex	$E_b(\text{eV})$			$d(\text{\AA})$		
	I	II	III	I	II	III
CNT- H_2P	0.84	1.01	1.01	3.26	3.13	3.15
CNT-ZnP	1.07	1.07	1.06	3.35	3.35	3.40
CNT- H_2Pc	1.50	1.52	1.56	3.21	3.15	3.26
CNT-ZnPc	1.55	1.55	1.58	3.27	3.27	3.23

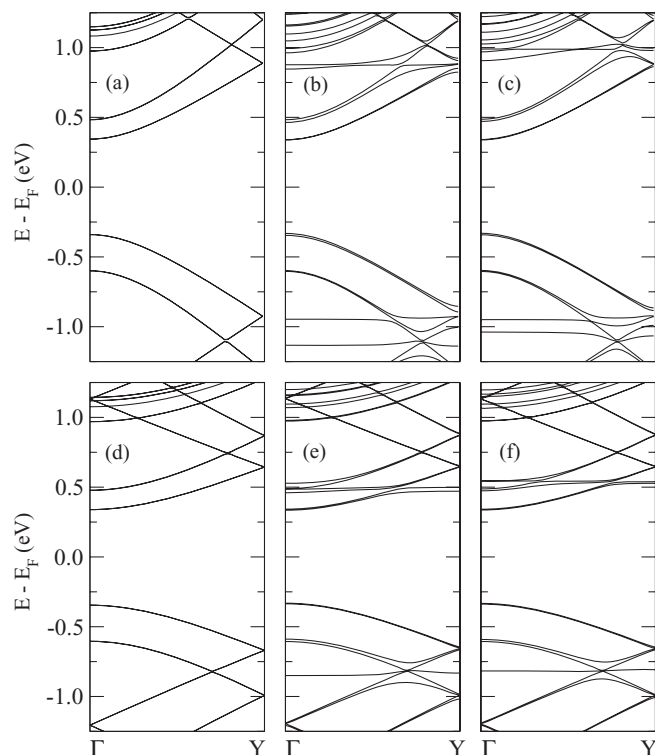


FIG. 2. Electronic bands structure of free-base and Zn macrocycles adsorbed on the CNT for a wave vector along the tube axis (ΓY). (a) Pristine CNT represented with four unit cell, (b) CNT-H₂P, (c) CNT-ZnP, (d) Pristine CNT represented with six unit cell, (e) CNT-H₂Pc, and (f) CNT-ZnPc.

parameter that increases the binding strength. We also found that the CNT geometry is almost unchanged with the presence of the porphyrins and phthalocyanines, which locate at around 3.1 and 3.3 Å from the CNT surface, respectively.

Figure 2 shows the band structures of pristine and functionalized CNTs for a wave vector along the CNT axis. For CNT-H₂P [Fig. 2(b)] and CNT-ZnP [Fig. 2(c)] we find very close electronic characteristics, suggesting similar optical properties for these complexes. The porphyrin higher occupied and lower unoccupied molecular orbitals (HOMO and LUMO) levels locate at around -1 and 1 eV with respect to the CNT Fermi energy, respectively. In the case of CNT-H₂Pc [Fig. 2(e)] and CNT-ZnPc [Fig. 2(f)], the molecular orbitals locates at around -0.8 and 0.5 eV. We can observe that the macrocycle interaction induces a slight symmetry breaking in the CNT band structure at the crossing points with the macrocycle molecular orbitals.

Figure 3 shows difference density plots for CNT-H₂Pc [Fig. 3(a)] and CNT-ZnPc [Fig. 3(b)] complexes. Here, the electronic density of the isolated CNT and the phthalocyanines, both frozen in the equilibrium geometry of the interacting systems, are subtracted from the electronic density of the complex, according to the equation:

$$\Delta\rho = \rho_{\text{CNT-ZnPc}} - (\rho_{\text{CNT}}^{\text{frozen}} + \rho_{\text{ZnPc}}^{\text{frozen}}). \quad (2)$$

Thus, $\Delta\rho$ indicates the charge displacement induced by the interaction between the molecule and the CNT. In Fig. 3, blue (red) isosurfaces cover regions where $\Delta\rho$ is negative

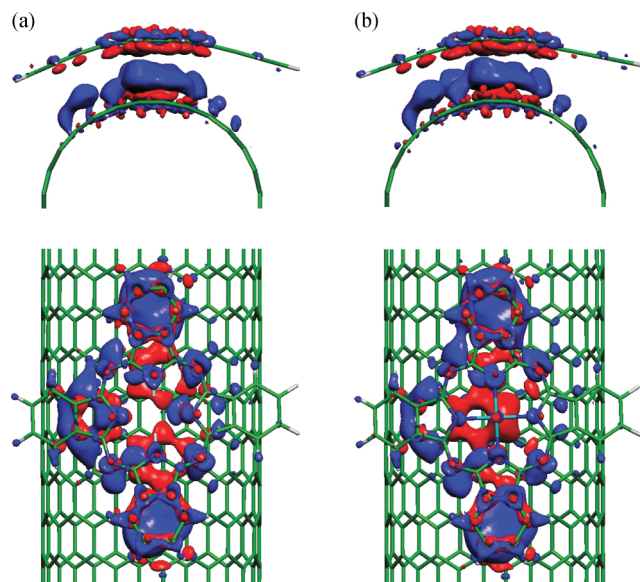


FIG. 3. (Color online) Charge density difference after the macrocycle adsorption on the CNT ($0.0002 e/\text{\AA}^3$). (a) CNT-H₂Pc and (b) CNT-ZnPc. Blue and red isosurfaces represent charge depletion and accumulation, respectively.

(positive), indicating charge density flows from the blue to the red regions when the phthalocyanine-CNT interaction is turned on. We observe a charge transfer from the complex interface to the CNT and to the macrocycle. For CNT-ZnPc the charge tends to locate around the Zn atom. Similar results are found for the porphyrins-CNT complexes. This charge redistribution indicates an electronic polarization at the adsorption site. Recent calculations show that the polarizability induced by adsorbates on semiconducting CNTs can redshift their exciton states.²³

B. Optical properties

The electronic absorption spectrum of porphyrins consist of a strong transition to the second excited state at about 400 nm (3.10 eV), the Soret or *B* band, and a weak transition to the first excited state at about 550 nm (2.25 eV), the *Q* band. Both the *B* and the *Q* bands arise from π - π^* transitions and can be characterized within a reasonably good approximation by considering only four frontier orbitals (HOMO-1, HOMO, LUMO, LUMO + 1), according to the Gouterman model.³⁰ This simple model has proved to be valid to describe the order and character of the energy levels of a free-base porphyrin when compared with more sophisticated theoretical approaches that include many-body perturbation theory.¹¹ Excitonic transitions associated with the *Q* bands are found to derive from a mixing of the single particle transitions from the HOMO to LUMO and from the HOMO to the LUMO + 1 levels, whereas those associated to the *B* bands are derived from HOMO-1 to LUMO and from HOMO-1 to LUMO + 1 levels. However, the *B* bands have additional contributions from HOMO-2 to LUMO + 1 transitions, which is not captured by the Gouterman model. Hence, the characterization of the *B* bands are expected to fail

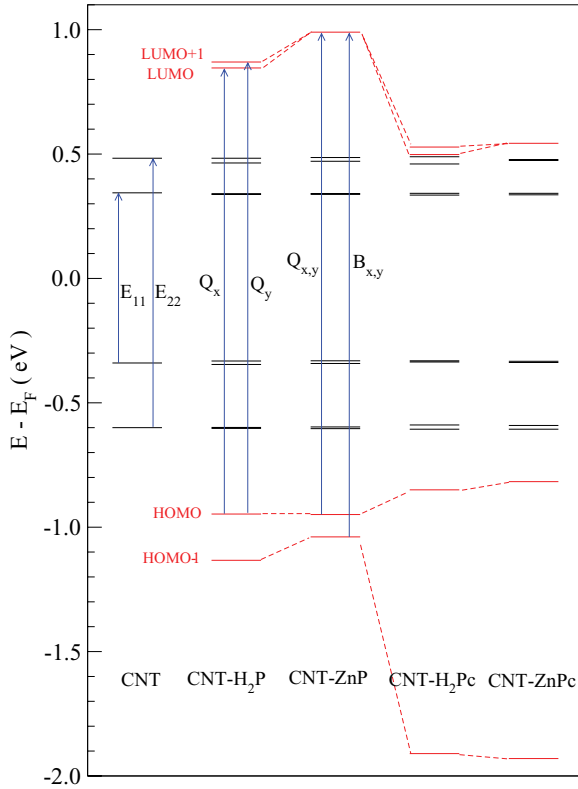


FIG. 4. (Color online) Schematic representation of energy levels and relevant optical transitions at the Γ point, according to the Gouterman model. The black (red) horizontal lines represent CNT (macrocycles) energy levels.

considering independent-particle calculations, and therefore will not be considered in the present work.

Figure 4 shows a schematic representation of the energy levels at the Γ point for the complex at the adsorption position III. Black lines represent CNT bands while the red ones macrocycles molecular orbitals. We find that for all macrocycles, the HOMO level is nondegenerated. For ZnP and ZnPc the LUMO level is double degenerated whereas for H₂P and H₂Pc this degeneracy is removed due to the breaking of the molecular symmetry by the exclusion of the metal center, resulting in two nondegenerated levels (LUMO and LUMO + 1). In Fig. 4, Q_x represents the HOMO-LUMO transition for the polarization of the incident light in the x direction. Similarly, Q_y represents the HOMO-LUMO + 1 transition for the polarization in the y direction. For the ZnP and ZnPc, Q_x and Q_y are the same due to the molecular symmetry. Table II summarizes our results for Q_x and Q_y optical transitions for the macrocycles under study as well as previous theoretical and experimental results. It is interesting to note that the molecular orbitals of the isolated macrocycles are almost unchanged when compared with those of the CNT-macrocycle complex, suggesting that the macrocycle absorption properties would be preserved after the interaction with the CNT.

Figure 5 shows the imaginary part of the dielectric function (ϵ_2) for the porphyrin-functionalized CNT: CNT-H₂P [Figs. 5(a)–5(c)] and CNT-ZnP [Figs. 5(d)–5(f)] in the two most stable geometries (positions II and III), considering

TABLE II. Optical transition energies for the isolated macrocycles. Q_x represents the transition between HOMO and LUMO and Q_y represents the transition between HOMO and LUMO + 1. Previous theoretical works and experiments are included for comparison.

Macrocycle	Method	Q_x (eV)	Q_y (eV)
H ₂ P	vdW-DF ^a	1.86	1.87
	GW-BSE ^b	1.98	2.30
	Expt. ^c	1.98–2.02	2.33–2.42
ZnP	vdW-DF ^a	1.99	1.99
	Expt. ^d	2.03	2.21
H ₂ Pc	vdW-DF ^a	1.35	1.39
	Expt. ^e	1.77	1.96
ZnPc	vdW-DF ^a	1.40	1.40
	Expt. ^e	1.80	1.98

^aThis work

^bReference 11.

^cReference 34.

^dReference 35.

^eReference 36.

polarizations for the incident light parallel to the CNT axis [Figs. 5(a) and 5(d)], perpendicular to the CNT axis in the direction x [Figs. 5(b) and 5(e)] and in the direction y [Figs. 5(c) and 5(f)]. The absorption of the isolated CNT are also depicted for comparison. In Figs. 5(a) and 5(d), the two peaks at around 1 eV correspond to the E_{11} and E_{22} transitions. We find that E_{11} is shifted toward the infrared by 10 meV with respect to the isolated CNT (see Table III), which is independent of the macrocycle adsorption position. Recent experiments have shown a similar redshift (~ 7 meV) in CNTs functionalized with porphyrins encased in micelles-composite materials.^{9,31–33} According to these works, the redshift is

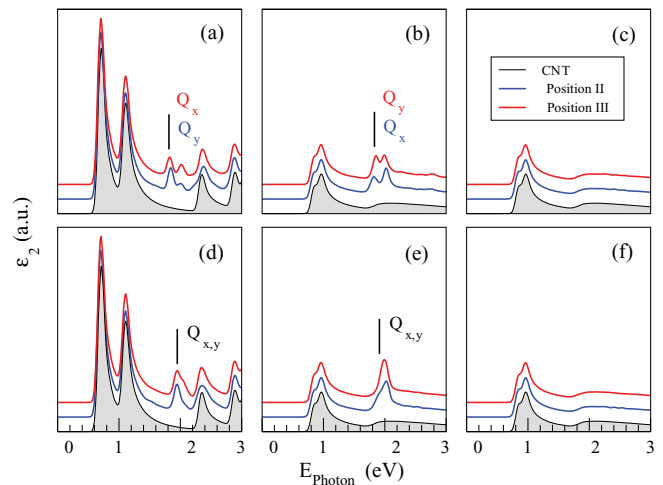


FIG. 5. (Color online) Imaginary part of the dielectric function of the CNT-H₂P [(a)–(c)] and CNT-ZnP [(d)–(f)] complexes as compared with the pristine CNT. Different polarization for the incident light are considered: (a) and (d) Incident light polarized parallel to the CNT axis. (b) and (e) Incident light polarized perpendicular to the CNT axis (x direction). (c) and (f) Incident light polarized perpendicular to the CNT axis (y direction). The vertical lines represent the position of the peaks associated to the Q bands.

TABLE III. Optical transition energies for the pristine and functionalized CNTs (in eV). E_{11} (E_{22}) represents the optical transition between the first (second) valence band and the first (second) conduction band. Q_x and Q_y represent the transitions associated to the adsorbed macrocycles.

Complex	E_{11}	E_{22}	Q_x	Q_y
CNT	0.71	1.11		
CNT-H ₂ P	0.70	1.10	1.82 (1.75) ^a	1.84
CNT-ZnP	0.70	1.10	1.95	1.95
CNT-H ₂ Pc	0.69	1.11	1.32	1.33
CNT-ZnPc	0.70	1.11	1.35	1.35

^aExpts. from Ref. 37.

associated to the interaction of porphyrins onto the CNT in close agreement with our results.

In the CNT-H₂P spectrum of Fig. 5(a), the presence of the macrocycle is detected by two peaks at around 1.8 and 2.0 eV, which can be associated to the Q and B bands, respectively. As we discuss above, the B band is not well described for the independent-particle approximation requiring the inclusion of many-body effects. In the present calculation the B band appears close to the Q band in the visible region, instead of the near ultraviolet. Because of this failure, we will focus only on the Q bands where the independent-particle approximation gives results much closer to the experimental ones, as shown by Palumbo *et al.*¹¹ For positions II and III, the Q peaks (at 1.8 eV) are labeled as Q_x and Q_y , which represent transitions for different polarization due to the rotation of the macrocycle by 45°. Figure 5(b) shows the spectrum for the polarization perpendicular to the CNT axis. Here we find the same behavior above described but with an exchange of the Q transitions due to the change in the light polarization. Figure 5(c) shows the spectrum for a polarization perpendicular to both the CNT axis and the plane of the macrocycle. Here we only observe CNT transitions without any macrocycle absorption, as expected due to the direction of the incident light. This result also tells us that the strong macrocycle distortion due to the interaction with the CNT do not induce any optical transitions in the molecule. For the CNT-ZnP complex [Fig. 5(d)], the Q_x and Q_y bands are degenerated due to the molecular symmetry, thus they are labeled as $Q_{x,y}$. We find that for both polarizations, parallel [Fig. 5(d)] and perpendicular [Fig. 5(e)] to the CNT axis, the $Q_{x,y}$ band locates at around 2.0 eV.

Figure 6 shows the imaginary part of the dielectric function for the phthalocyanine-functionalized CNT: CNT-H₂Pc [Figs. 6(a)–6(c)] and CNT-ZnPc [Figs. 6(d)–6(f)]. Here we find that for light polarized parallel and perpendicular to the CNT axis, the Q bands locate at the same place, around 1.4 eV, showing a dislocation of about 0.6 eV with respect to those found in the porphyrin-functionalized CNT. This shift suggests that porphyrins and phthalocyanines on CNTs would absorb at different sites in the solar radiation spectrum, following the same trend as the isolated macrocycles. Therefore, a solar-energy conversion device based on noncovalent functionalized semiconducting CNTs would have higher efficiency if both porphyrins and phthalocyanines are simultaneously adsorbed on the CNT sidewall.

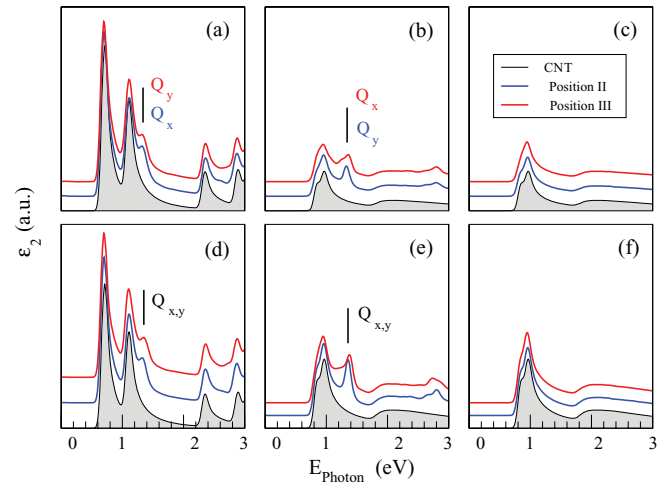


FIG. 6. (Color online) Imaginary part of the dielectric function for the CNT-H₂Pc [(a)–(c)] and CNT-ZnPc [(d)–(f)] complexes as compared with the pristine CNT. Different polarization of the incident light are considered: (a) and (d) Incident light polarized parallel to the CNT axis. (b) and (e) Incident light polarized perpendicular to the CNT axis (x direction). (c) and (f) Incident light polarized perpendicular to the CNT axis (y direction). The vertical lines represent the position of the peaks associated to the Q bands.

According to recent photoluminescence experiments in noncovalently bound CNT-porphyrin assemblies, when a photon is absorbed by the porphyrin, the luminescence of the CNT is enhanced, showing unambiguous evidence of excitation energy transfer from the porphyrin to the CNT.⁹ This phenomenon is believed to occur by the dipole-dipole coupling between the CNT and the adsorbed molecules without exchange of photons in a process known as Förster resonance energy transfer.³⁸ The resonance can take place when a donor molecule (fluorophore), in an electronically excited state, transfers its excitation energy to a nearby acceptor molecule (chromophore). In Fig. 3 we find a redistribution of charge at the CNT-macrocycle interface, indicating a local dipole-dipole interaction. This dipole interaction and the small spacing at the CNT-macrocycle interface suggests that the highly efficient excitation energy transfer observed in CNT-porphyrin assemblies⁹ would be originated in a resonance energy transfer process.

IV. SUMMARY AND CONCLUSIONS

In summary, we have studied the structural, electronic, and optical properties of free-base and Zn porphyrins and phthalocyanines physisorbed on semiconducting CNTs, using *ab initio* calculations. The macrocycle physisorption is described by van der Waals density functional while the response of the functionalized CNT to light polarized both parallel and perpendicular with respect to the CNT axis is investigated through the imaginary part of the dielectric function in the linear optical response. Our results indicate a strong macrocycle adsorption energies on the CNT sidewall, around 1.0 eV for porphyrins and 1.5 eV for phthalocyanines, but with negligible effects on the CNT geometry and the band structures, suggesting that the CNT high mobility would be preserved after the functionalization. Comparing the E_{11}

optical transition of the pristine CNT with the functionalized CNT we observe a redshift for the latter of about 10 meV, which is attributed to a polarization effect induced by the adsorbate, in close agreement with previous theoretical and experimental results.^{21,23} Concerning the CNT-macrocycle optical properties, we find that for light polarizations parallel and perpendicular to the CNT axis, the Q band locates at 1.8 and 2.0 eV for H₂P and ZnP, respectively, whereas for H₂Pc and ZnPc it locates at the same energy, 1.4 eV. These results suggest that a CNT functionalized with both porphyrins

and phthalocyanines would absorb at different energies in the visible solar radiation spectrum, which would enhance the efficient use of sunlight for photovoltaic applications. Finally, we believe that future calculations including many-body effects could be important to confirm our results.

ACKNOWLEDGMENTS

This work was supported by FONDECYT under Grants No. 3110123 and No. 1090489.

- ¹C. Ehli, C. Oelsner, D. M. Guldi, A. Mateo-Alonso, M. Prato, C. Schmidt, C. Backes, F. Hauke, and A. Hirsch, *Nat. Chem.* **1**, 243 (2009).
- ²E. Malic, C. Weber, M. Richter, V. Atalla, T. Klamroth, P. Saalfrank, S. Reich, and A. Knorr, *Phys. Rev. Lett.* **106**, 097401 (2011).
- ³J. H. Zagal, S. Griveau, K. I. Ozoemena, T. Nyokong, and F. Bedioui, *J. Nanosci. Nanotechnol.* **9**, 2201 (2009).
- ⁴W. Orellana, *Phys. Rev. B* **84**, 155405 (2011).
- ⁵W. Orellana, *Chem. Phys. Lett.* **541**, 81 (2012).
- ⁶F. D'Souza, S. D. Sandanayaka, and O. Ito, *J. Phys. Chem. Lett.* **1**, 2586 (2010).
- ⁷J. Bartelmess, B. Ballesteros, G. de la Torre, D. Kiessling, S. Campidelli, M. Prato, T. Torres, and D. M. Guldi, *J. Am. Chem. Soc.* **132**, 16202 (2010).
- ⁸J. Gupta, C. Vijayan, S. K. Maurya, and D. Goswami, *J. Appl. Phys.* **109**, 113101 (2011).
- ⁹C. Roquelet, J.-S. Lauret, V. Alain-Rizzo, C. Voisin, R. Fleurier, M. Delarue, D. Garrot, A. Loiseau, P. Roussignol, J. A. Delaire, and E. Deleporte, *ChemPhysChem* **11**, 1667 (2010).
- ¹⁰D. M. Guldi, G. M. A. Rahman, N. Jux, N. Tagmatarchis, and M. Prato, *Angew. Chem., Int. Ed. Engl.* **43**, 5526 (2004).
- ¹¹M. Palummo, C. Hogan, F. Sottile, P. Bagalá, and A. Rubio, *J. Chem. Phys.* **131**, 084102 (2009).
- ¹²G. Stenuit, C. Castellarin-Cudia, O. Plekan, V. Feyer, K. C. Prince, A. Goldoni, and P. Umari, *Phys. Chem. Chem. Phys.* **12**, 10812 (2010).
- ¹³X. Blase, C. Attaccalite, and V. Olevano, *Phys. Rev. B* **83**, 115103 (2011).
- ¹⁴N. Marom, X. Ren, J. E. Moussa, J. R. Chelikowsky, and L. Kronik, *Phys. Rev. B* **84**, 195143 (2011).
- ¹⁵M. Machón, S. Reich, C. Thomsen, D. Sánchez-Portal, and P. Ordejón, *Phys. Rev. B* **66**, 155410 (2002).
- ¹⁶Y. Takagi and S. Okada, *Phys. Rev. B* **79**, 233406 (2009).
- ¹⁷T. H. Cho, W. S. Su, T. C. Leung, W. Ren, and C. T. Chan, *Phys. Rev. B* **79**, 235123 (2009).
- ¹⁸C. D. Spataru, S. Ismail-Beigi, L. X. Benedict, and S. G. Louie, *Phys. Rev. Lett.* **92**, 077402 (2004).
- ¹⁹G. Dukovic, F. Wang, D. Song, M. Y. Sfeir, T. F. Heinz, and L. E. Brus, *Nano Lett.* **5**, 2314 (2005).
- ²⁰H. Lin, J. Lagoute, V. Repain, C. Chacon, Y. Girard, J.-S. Lauret, F. Ducastelle, A. Loiseau, and S. Rousset, *Nat. Mater.* **9**, 235 (2010).
- ²¹P. Finnie, Y. Homma, and J. Lefebvre, *Phys. Rev. Lett.* **94**, 247401 (2005).
- ²²F. Wang, M. Y. Sfeir, L. Huang, X. M. Henry Huang, Y. Wu, J. Kim, J. Hone, S. O'Brien, L. E. Brus, and T. F. Heinz, *Phys. Rev. Lett.* **96**, 167401 (2006).
- ²³M. Rohlfing, *Phys. Rev. Lett.* **108**, 087402 (2012).
- ²⁴J. M. Soler, E. Artacho, J. D. Gale, A. Garcia, J. Junquera, P. Ordejón, and J. D. Sánchez-Portal, *J. Phys.: Condens. Matter* **14**, 2745 (2002).
- ²⁵M. Dion, H. Rydberg, E. Schröder, D. C. Langreth, and B. I. Lundqvist, *Phys. Rev. Lett.* **92**, 246401 (2004).
- ²⁶S. D. Chakarova-Käck, E. Schröder, B. I. Lundqvist, and D. C. Langreth, *Phys. Rev. Lett.* **96**, 146107 (2006).
- ²⁷I. Ruiz-Tagle and W. Orellana, *Phys. Rev. B* **82**, 115406 (2010).
- ²⁸R. B. Weiman and S. M. Bachilo, *Nano Lett.* **3**, 1235 (2003).
- ²⁹W. Orellana, R. H. Miwa, and A. Fazzio, *Surf. Sci.* **566**, 728 (2004).
- ³⁰M. Gouterman, *J. Chem. Phys.* **30**, 1139 (1959); M. Gouterman, G. Wagniere, and L. C. Synder, *J. Mol. Spectrosc.* **11**, 108 (1963); C. Weiss, H. Kobayashi, and M. Gouterman, *ibid.* **16**, 415 (1965).
- ³¹G. Magadur, J.-S. Lauret, V. Alain-Rizzo, C. Voisin, P. Roussignol, E. Deleporte, and J. A. Delaire, *ChemPhysChem* **9**, 1250 (2008).
- ³²S. Cambré, W. Wenseleers, J. Culin, S. Van Doorslaer, A. Fonseca, J. B. Nagy, and E. Goovaerts, *ChemPhysChem* **9**, 1930 (2008).
- ³³S. Berger, F. Iglesias, P. Bonnet, C. Voisin, G. Cassaboïs, J.-S. Lauret, C. Delalande, and P. Roussignol, *J. Appl. Phys.* **105**, 094323 (2009).
- ³⁴L. Edwards, D. H. Dolphin, M. Gouterman, and A. D. Adler, *J. Mol. Spectrosc.* **38**, 16 (1971).
- ³⁵M. P. Pileni and M. Graetzel, *J. Phys. Chem.* **84**, 1822 (1980).
- ³⁶R. Seoudi, G. S. El-Bahy, and Z. A. El Sayed, *Opt. Mater.* **29**, 304 (2005).
- ³⁷J. Chen and C. P. Collier, *J. Phys. Chem. B* **109**, 7605 (2005).
- ³⁸A. Ahmad, K. Kern, and K. Balasubramanian, *ChemPhysChem* **10**, 905 (2009).